http://dx.doi.org/10.5012/bkcs.2013.34.1.231

Simple Analysis for Interaction between Nanoparticles and Dye-Containing Vesicles as a Biomimetic Cell-Membrane

Sohyang Shin, Ha Nee Umh, and Younghun Kim*

*Department of Chemical Engineering, Kwangwoon University, Seoul 151-742, Korea. *E-mail: korea1@kw.ac.kr*
Received October 4, 2012, Accepted November 5, 2012

Some cytotoxicity studies for the interpretation of the interaction between nanoparticles and cells are non-mechanistic and time-consuming. Therefore, non-biological screening methods, which are faster and simpler than *in-vivo* and *in-vitro* methods, are required as alternatives to current cytotoxicity tests. Here, we proposed a simple screening method for the analysis of the interaction between several AgNPs (bare-, citrate-, and polyvinylpyrrolidone-coating) and dye-containing vesicles acting as a biomimetic cell-membrane. The interaction between AgNPs and vesicles could be evaluated readily by UV-vis spectra. Absorbance deviation in UV-vis spectra revealed a large attraction between neighboring particles and vesicles. This was confirmed by (Derjagin, Landau, Verwey, and Overbeek) theory and DMF (dark-field microscopy) analysis. This proposed method might be useful for analyzing the cytotoxicity of nanoparticles with cell-membranes instead of in vitro or in vivo cytotoxicity tests.

Key Words : Silver nanoparticles, Toxicology, Biomimetic, Vesicle, Dark field microscopy

Introduction

Toxicity test for new chemicals was mainly carried out by high-dose testing for extrapolation from high to lower doses and from the experimental animals to the human population.[1-3] This test is expensive, time-consuming, and characterized by low-throughput and questionable relevance to predicting risks to humans at low exposures and to understanding cytotoxicity mechanisms. Therefore, an alternative vision proposed by the U.S. National Research Council called for moving away from traditional high-dose animal studies to an approach based on the perturbation of cellular responses using well-designed *in-vitro* assays.[4]

Concerns for the environmental, health and safety risks of nanoparticles have recently emerged, and notably, silver nanoparticles (AgNPs), as a strong antibiotic material, were found to cause cell necrosis. It has come to light that nanoparticles might induce hazardous effects on bio-organisms by direct damage to cell membranes, and may cause cell rupture, adsorption on the membrane, or generation of reactive oxygen species.[5,6] Therefore, *in-vivo* and *in-vitro* cytotoxicity testing for nanoparticles, referred to as new chemicals by REACH (Registration, Evaluation, Authorization and Restriction of Chemicals), has been necessary to quantify and qualify their nanotoxicity.[7-9] However, these cytotoxicity tests for nanoparticles are not suitable for rapidly screening the various nanoparticles used in industrial applications. Therefore, non-biological screening methods, which are faster and simpler than *in-vivo* and *in-vitro* methods, are required as alternatives to current cytotoxicity tests.[10,11]

Phospholipid layers are well-defined models for cell surfaces and for investigating molecular events in the membrane.[12-14] Recently, Shiraki group suggested a simple test method for adsorption and disruption of lipid bilayers by nanoscale protein aggregation.[12] Frank and co-worker investigated what happens when POPC (1-palmitoyl-2-oleoyl-*sn*-glycero-3-phosphocholine) vesicles are exposed to the amphipathic helix peptide.[13] Chah and Zare presented evidence that the POPC vesicles transform into a lipid bilayer using *in-situ* SPR (surface plasmon resonance).[14] A mimetic lipid vesicle could be used as a well-designed testing tool for understanding the interaction between nanoparticles and cell-membranes, and rapidly screening the direct damage to cells from adsorption of nanoparticles and cell rupture.

To define the interaction between nanoparticles and vesicles, SPR or TEM (transmission electron microscopy) analysis is usually used. Herein, we suggest a more efficient and simple method to analyze the adsorption of nanoparticles on vesicles by UV-vis spectroscopy. Because vesicles are transparent and not detectable by a UV photometer, dye-containing vesicles were prepared using dye molecules. DMPG (1,2-dimyristoyl-*sn*-glycero-3-[phosphor-rac-glycerol]) vesicles in chloroform were dried under an N_2 stream and re-suspended in a mixture of PBS (phosphate buffered saline) and Acid Red 44 ($C_{20}H_{12}N_2Na_2O_7S_2$). After centrifugation, dye-containing vesicles were finally obtained with diameters of about 1-5 μm.

Experimental

Preparation of Dye-Contained Vesicle. The sodium salt of the phospholipd DMPG was purchased from Avanti Polar Lipids. A chloroform lipid solution was spread on the rough side of a Teflon disk, which was kept under reduced pressure overnight to remove all traces of organic solvent. In a prehydration stage, a bottle was left in a humid atmosphere for 2 h at 37 °C.[15] After that, 4 mL of a mixture solution of 1xPBS and 400 ppm of Acid Red 44 was gently poured into

the bottle. The bottle was closed with a cap and left at 37 °C for 2 days. After centrifugation at 4000 rpm for 4 min, the supernatant was discarded to remove the rest of the dye and the final material was re-dispersed in the PBS solution. The final lipid concentration was smaller than 40 μM, because it is not known whether all lipids left the Teflon surface to form vesicles.

Preparation of Bare-AgNPs. A nano-silver powder (Sigam-Aldrich, 99%, < 100 nm) without suspension additives was prepared as a suspension of AgNPs in an aqueous phase *via* THF (tetrahydrofuran) method,[16] which can be readily exchanged with water and is easily removed by evaporation. Ag powder was added to THF and the resulting solution was treated with sonication, followed by stirring at approximately 300 rpm until the THF had completely evaporated (1-2 days). Deionized (DI) water was added to replace the THF. The resulting sample was then filtered through a polycarbonate membrane filter (50 nm isopoere, Adventec).

Preparation of Citrate-AgNPs. Citrate-coated AgNPs were prepared by a drop-wise method that added 0.6 mL of 7 mM $NaBH_4$ (Sigma-Aldrich) solution to 1 mL of 26 mM $AgNO_3$ (Sigma-Aldrich) in 19 mL of 1 mM trisodium citrate (Sigma-Aldrich) under vigorous stirring. The color of the solution immediately changed to dark yellow after the $NaBH_4$ was added, which indicated particle formation. After 2 h, this solution was subjected to centrifugation at 13000 rpm for 15 min.

Preparation of PVP (polyvinylpyrrolidone)-AgNPs. 9 mL of 0.1 M silver nitrate was added to 280 mL of 5.36 g/L aqueous PVP suspension while stirring.[17] After stirring for 5 min, 11 mL of 0.08 M sodium borohydride was then added to the solution and stirred for 10 min. The PVP-AgNPs were ultracentrifuged at 14,000 rpm, then re-suspended in water.

Characterizations. Particle size and zeta potential were measured by electrophoretic light scattering (ELS-Z, Otsuka). UV-vis spectra were analyzed with a UV-vis spectrophotometer (UV-1800, Shimadzu). Dark-field images were analyzed with dark-field microscopy (DFM, Axio Observer Z1, Carl Zeiss) and light-scattering images were collected using a CCD camera (AxioCam MRc 5, Carl Zeiss). The TEM image of the vesicles and AgNPs were analyzed with transmission electron microscopy (JEM 1010, JEOL).

Results and Discussion

Generally, a cell-membrane has a negative charge, and thus, DMPG with a negative charge was selected as biomimetic cell-membrane. Three different AgNPs were selected as target nanoparticles: i) bare-AgNPs without any additives, ii) citrate-AgNPs with a citrate coating, and iii) PVP-AgNPs with a PVP (polyvinylpyrrolidone) coating. Their sizes were measured by ELS (electrophoretic light scattering) and TEM analysis (Fig. 1). These AgNPs had different surface charges, and thus show different interactions with the dye-containing vesicles. Differences of interaction between the x-AgNPs and the vesicles affect the absorbance of UV spectra.

As shown in Figure 2(a), x-AgNPs were absorbed or separated from the vesicles after exposure, depending on the intensity of the electrostatic charge repulsion. While the absorbance for the mixture of vesicles and bare-AgNPs gradually increased until 2 h, that for citrate-AgNPs gradually decreased, and PVP-AgNPs was less changed. If no interactions between the vesicles and the AgNPs, spectra **4** (mixture of vesicles and AgNPs) in Figure 2(b) would be the

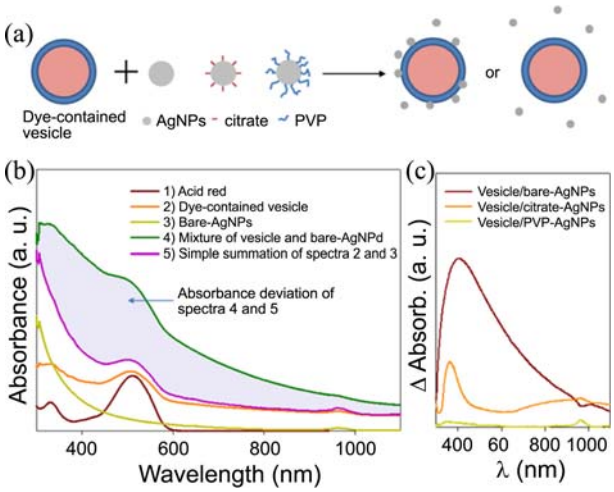

Figure 2. (a) Schematic illustration of interaction between dye-contained vesicle and various AgNPs. (b) UV-vis spectra for interaction between vesicle and bare-AgNPs. (c) Absorbance deviation between spectra 4 and 5, namely, colored area in figure (b). Where, x is bare, citrate, and PVP.

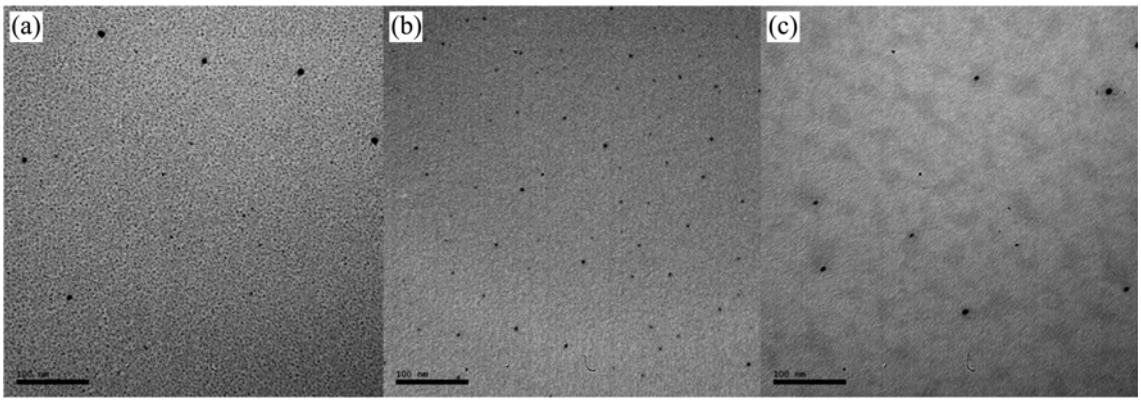

Figure 1. TEM images of (a) bare-, (b) citrate-, and (c) PVP-AgNPs (1 bar = 100 nm).

Table 1. Characteristic properties of dye-containing DMPG vesicle and x-AgNPs

Materials	C/ppm	R/nm	t/nm	d/nm	ξ/mV
Vesicle	40	943	3.1	$>10^4$	−39.8
Bare-AgNPs	50	2.8	~0	61	+32.5
Citrate-AgNPs	50	2.0	~0	22	−38.9
PVP-AgNPs	50	3.5	2.6	634	−5.0

*C: concentration in solutions; R: radius of particles (measured by TEM and ImageJ software); t: thickness of lipid bilayer or coating materials on AgNPs; d: interparticle distance between neighboring particles; ξ: zeta potential of particles.

same as spectra **5** (simple summation of spectra of vesicles and AgNPs). Since the total intensity is dependent on the individual absorbance (ψ), the following relation is reasonable for interpretation of the particle interaction:

$$[\psi_{ves}]^2 + [\psi_{Ag}]^2 = [\psi_{ves} + \psi_{Ag}]^2 \text{ for non-interaction} \quad (1)$$

$$[\psi_{ves}]^2 + [\psi_{Ag}]^2 [\psi_{ves} + \psi_{Ag}]^2 \text{ for interaction} \quad (2)$$

However, absorbance deviation was found in the mixture of vesicles and bare-AgNPs, as shown in Figure 2(b). The deviation is large for bare-AgNPs but small for citrate- and PVP-AgNPs (Fig. 2(c)). The maximum deviations were 397 and 362 nm for bare- and citrate-AgNPs, respectively. The spectra area of absorbance deviations for bare-, citrate-, and PVP-AgNPs were 126, 40, and 3, respectively. And its spectra area of absorbance deviation for bare-, citrate-, and PVP-AgNPs is 126, 40, and 3, respectively. AgNPs are well-known for their localized surface plasmon resonance (LSPR) properties, which originate from collective oscillation of their electrons in response to optical excitation.[18] In general, spherical AgNPs with a size of about 10 nm size have an LSPR peak around 400 nm. Therefore, a maximum peak in deviation spectra is induced by this LSPR phenomenon. In addition, by the Beer-Lambert law, changes of the refractive index were affected by the absorptivity, and thus, the refractive index of the vesicle/bare-AgNPs system might be increased before mixing the vesicle and bare-AgNPs. The absorbance intensity is affected by the ensemble effect between vesicles and AgNPs. In the case of bare-AgNPs, this effect is larger than other AgNPs due to small electrostatic repulsion.

In addition, the separation distance between particles affects the absorbance deviation, and that between vesicles and bare-AgNPs might be close to each other, but are large for PVP-AgNPs. The importance of interparticle interactions can be deduced from the values of the interparticle distance (d) and the Debye length.[19] Debye length in colloidal dispersion is dependent on the ionic strength (I) of the electrolyte, which was calculated as 0.76 nm for the ca. 0.2 M PBS used in this study. Based on the simple spherical model,[20] the interparticle distance can be estimated as in Table 1.

$$d_{vesicle} = \sqrt[3]{\frac{4\pi/3[R^3-(R-t_b)^3]}{C}} \quad (3)$$

Where, R, t_b, and C are radius, lipid thickness, and concentration of vesicle, respectively.

$$d_{AgNPs} = \sqrt[3]{\frac{4\pi/3(R^3+t)^3}{C}} \quad (4)$$

Where, t is the thickness of the coating materials (*i.e.* citrate and PVP) on the surface of the AgNPs.

The concentrations of the vesicles and AgNPs are quite diluted, and thus, the intervesicular distance between vesicles is large ($> 10^4$ nm). The layer thickness (t) of DMPG (lipid bilayer) and PVP-AgNPs (PVP coating) was cited in reported data.[17] In contrast, the d value was smaller than that of vesicles, because x-AgNPs are small (*ca.* 4-7 nm). The interparticle distance of the bare-AgNPs is three times larger than citrate-AgNPs (22 nm) and smaller than PVP-AgNPs (634 nm). The Debye length for this system was comparable to ($d_{particle}$-$2R_{particle}$) in Table 1, the typical separation between two neighboring particles. Weak interparticle interactions are present at these concentrations. Therefore, the interparticle distance of individual particles is enough for them to separate fully from each other stably in solutions before mixing with vesicle and x-AgNPs.

The electrostatic force depends on the zeta potential (ξ) and thickness of the electrical double layer (Debye length, 1/κ), and is calculated by classical DLVO (Derjagin, Landau, Verwey, and Overbeek) theory for two spherical particles and steric interaction.[21-23] The total interaction energy (V_T) is defined as the sum of attractive van der Waals (V_A) and repulsive electric double layer interactions (V_R), and additional steric hindrance (V_S) for PVP-AgNPs.

$$V_A = -\frac{A_{132}}{6}\left(\frac{r_1 r_2}{r_1+r_2}\right)\frac{1}{D} \quad (5)$$

Where, r_i and D are the radius of particles and the distance between particles, respectively. A_{132} is the Hamaker constant, *i.e.* attraction parameter.

$$V_R = 64\pi\varepsilon\varepsilon_r\gamma_1\gamma_2\frac{r_1 r_2}{r_1+r_2}\left(\frac{kT}{ve}\right)^2\exp(-\kappa D)$$

$$\text{with } \gamma_i = \tanh\left(\frac{ve\xi_i}{4kT}\right) \quad (6)$$

Where, ε, ε_r, k, e, T, ξ and κ are vacuum permittivity (8.854×10^{-12} F/m), solvent dielectric constant (80.4), Boltzmann constant (1.381×10^{-23} m^2kg/s^2K), electronic charge (1.602×10^{-19} C), temperature (298.15 K), zeta potential of particles, and inverse Debye length, respectively.

$$V_S = 4\pi r kT(0.5-\aleph)\Gamma^2\exp\left(1-\frac{D}{2t}\right) \quad (7)$$

Where χ, Γ and t are the Flory polymer/solvent interaction parameter (~0.5 for PVP/water), adsorbed amount (2.8-8.4 mg/m^2), and layer thickness (2.6 nm), respectively.

The attraction parameter, Hamaker constant (A_{132}), which is represented in interacting media such as vesicle-water-

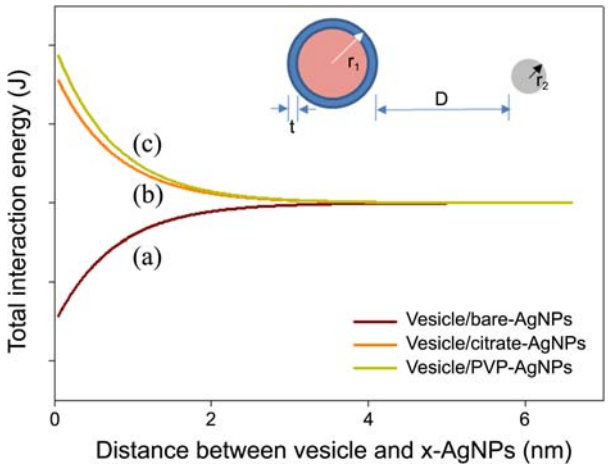

Figure 3. Total interaction energy profile between dye-contained vesicle and (a) bare-, (b) citrate-, and (c) PVP-AgNPs.

AgNPs, is needed for the calculation of the van der Waals interaction. These values for Ag, DMPG, water, citrate-AgNP and polymer were selected as 3.85×10^{-19}, $8\text{-}10 \times 10^{-21}$, 3.7×10^{-20}, 3.5×10^{-20}, and $4\text{-}7 \times 10^{-20}$ J, based on the reported data.[17,24-26] The V_A between vesicles and x-AgNPs has the negatively largest value for bare-AgNPs at -10^{-19} J, compared to the citrate-AgNPs (-10^{-21} J) and PVP-AgNPs (-10^{-20} J). The zeta potential of the particles was used to analyze the electrostatic repulsion (V_R) in γ values. When the zeta potentials of two neighboring particles are the same, V_R has a positive value as repulsion energy. Due to the opposite zeta potentials between DMPG vesicles (–39.8 mV) and bare-AgNPs (+32.5 mV), there was a great attraction force, and the total interaction energy was revealed as a negative attraction (Fig. 3(a)). In contrast, the total energy for vesicle/citrate-AgNPs showed positive repulsion (Fig. 3(b)). PVP-AgNPs are stabilized in solutions by two mechanisms: Coulombic and steric repulsion. Therefore, V_S is further considered to calculate total interaction energy. In the V_S equation, the Flory PVP/water parameter was selected as ~0.5.[27] Contribution of steric hindrance is small, compared to electrostatic repulsion, and thus V_T for vesicle/PVP-AgNPs had a slightly larger repulsive force than vesicle/citrate-AgNPs. Therefore, bare-AgNPs can absorb strongly on vesicles, and thus change the refractive index in UV spectra, as shown in Figure 2(c).

As described in the introduction,[12-14] SPR analysis is a powerful tool for the molecular level detection of inorganic/organic loading on a gold chip. The reflectivity (Fig. 4) was measured in real time as we changed the conditions on a gold surface. The reflectance of the bare gold chip was found to have drastically increased by 20% (R/R_o) when dye-containing vesicles were injected into the cell. After injection of x-AgNPs onto a vesicle/gold chip, the reflectances for the x-AgNPs were changed in different ways for each sample. Citrate- and PVP-AgNPs increased their R/R_o value, but bare-AgNPs decreased slightly in reflectance, as compared to only loading vesicles on the gold chip. In general, AgNPs

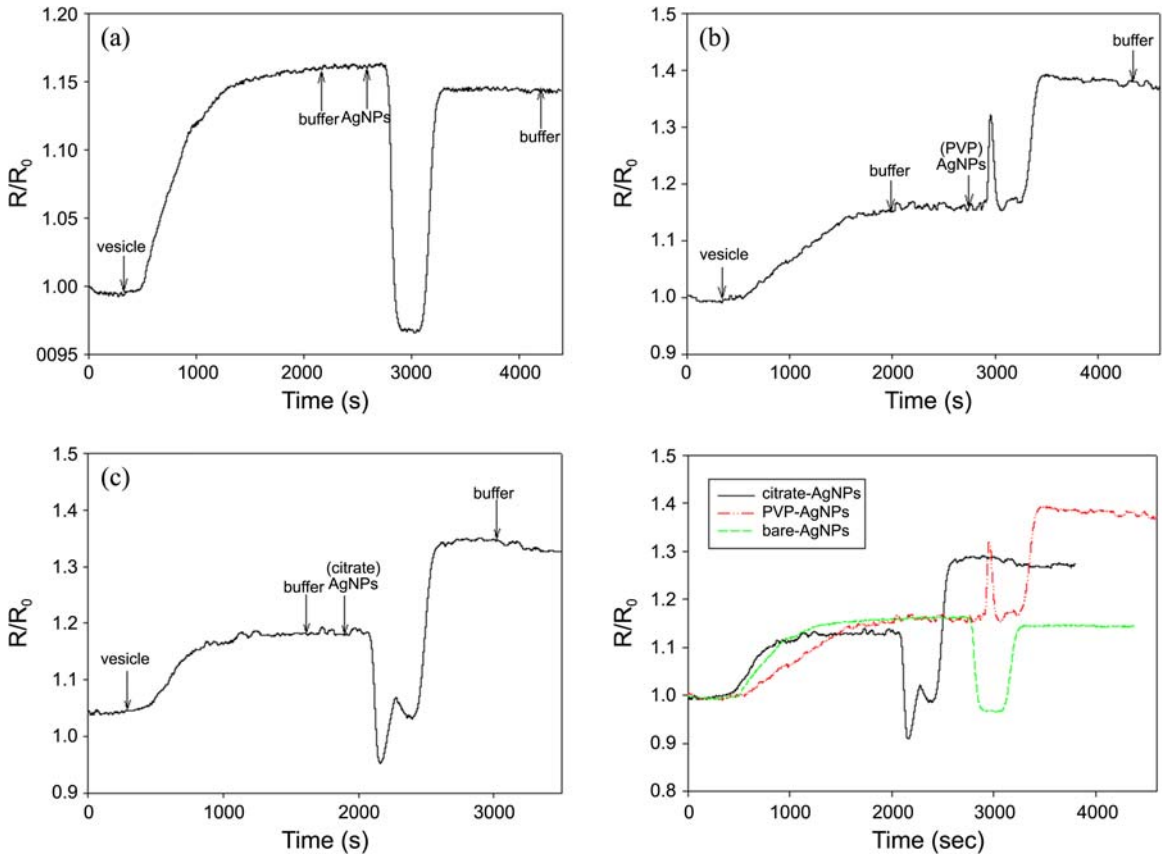

Figure 4. Time-resolved SPR responses for (a) bare-, (b) citrate-, and (c) PVP-AgNPs injection on vesicle/Au chip, with PBS buffer system.

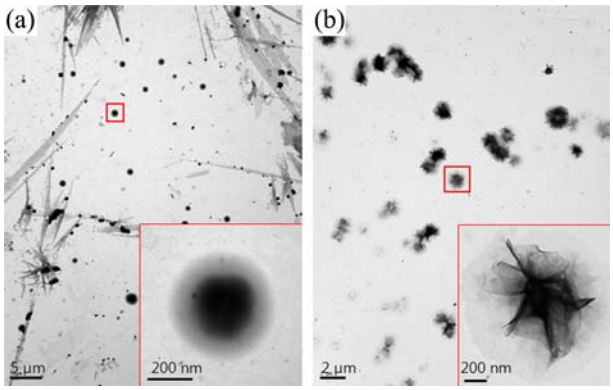

Figure 5. TEM images for (a) dye-contained vesicle and (b) vesicle/bare-AgNPs (after AgNPs exposure).

enhanced the reflectance value on the gold chip, and citrate- and PVP-AgNPs had an increased R/R_o value. However, in this case, bare-AgNPs with vesicles decreased the R/R_o value. Therefore, bare-AgNPs affect the vesicle adsorption on gold chips, and vesicles flow down loosely with bare-AgNPs. It is noted that the increasing of refractance in the UV-vis spectra enhanced the absorptivity, while a slight decrease of reflectance revealed the detachment of vesicles loosely with AgNPs in the flow of buffer.

To verify the morphological changes of dye-containing vesicles after the addition of bare-AgNPs, TEM and DFM (dark-field microscopy) analysis were carried out. In the TEM image (Fig. 5), dye-containing vesicles were spherical before the addition of bare-AgNPs, whereas the surfaces of the vesicles were wrinkled and shrunk after the addition. The bare-AgNPs affected the surface morphology of vesicles. However, the TEM image was obtained after drying the colloidal sample on a TEM Cu-grid, and thus the drying process would have changed the morphology of the vesicle/bare-AgNPs. Therefore, DFM images were obtained in liquid media as shown in Figure 6. Metallic nanoparticles scatter light intensely, and they are much brighter than chemicals in aqueous phase. They do not photobleach and can be easily detected at the single-particle limit.[28] Plasmonic nanoparticles exhibited enhanced scattering at wavelengths of their localized plasmon resonance.

Figure 6(a) shows a light scattering image of the representative dye-containing vesicles, and its colors are dim blue and green, which was revealed only in the bilayer. Bare-AgNPs (Fig. 6(b)), citrate-AgNPs (Fig. 6(e)), and PVP-AgNPs (Fig. 6(g)) in DFM images showed intense spherical scattering light. The particle colors were mostly blue and green. The color indexes for blue, green and red generally correspond to size indexes of 50 ± 10, 70 ± 10, and 90 ± 10 nm, respectively.[29] Therefore, the sizes of the x-AgNPs can be presumed to be in a size under 40-80 nm. The vesicles had no bright color intensity compared to the AgNPs, and vesicles after mixing with bare-AgNPs showed bright color at their bilayer zones, as shown in Figure 6(c). In a magnified image (Fig. 6(d)), bare-AgNPs were close to the surface of the AgNPs and partially adsorbed. Thus, AgNPs on the

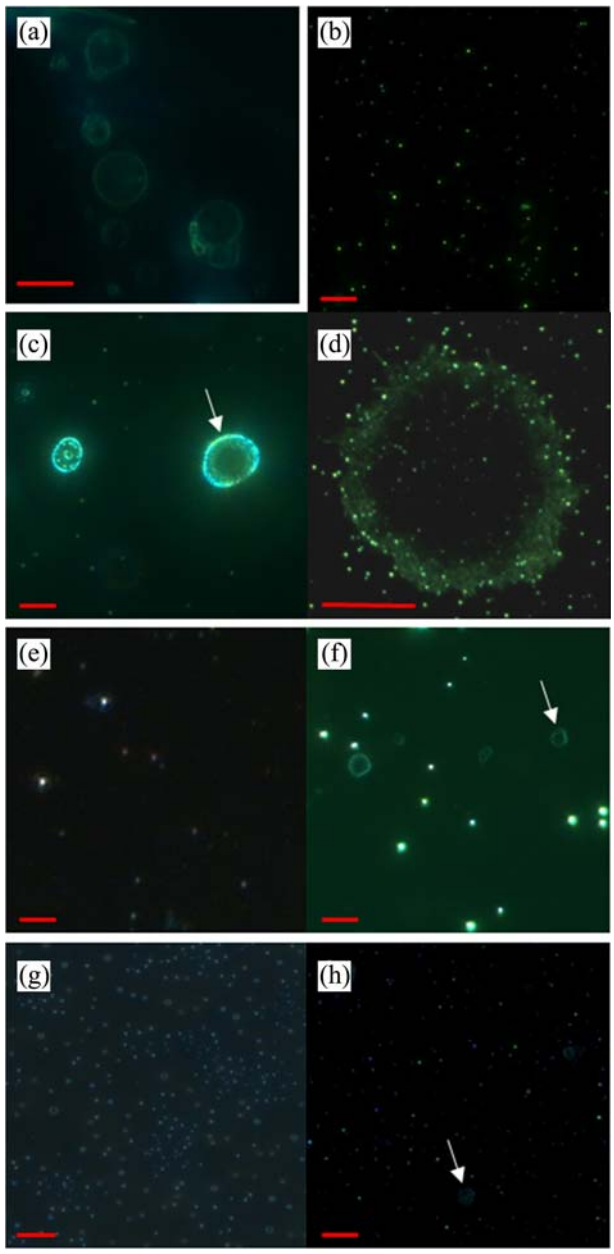

Figure 6. DFM images for vesicles and mixture of vesicles-AgNPs. (a) Giant DMPG vesicle, (b) bare-AgNPs, (c) mixture of vesicle and bare-AgNPs, (d) magnification of (c), (e) citrate-AgNPs, (f) mixture of vesicle and citrate-AgNPs, (g) PVP-AgNPs, and (h) mixture of vesicle and PVP-AgNPs (Scale bar = 5 μm).

outer surface of the vesicles revealed intense light scattering. However, vesicles with citrate- and PVP-AgNPs had no bright light scattering on the vesicle surface. As shown in Figures 6(f) and 6(h), the vesicles showed very dim color compared to the AgNPs. It is noted that the AgNPs were not attached on the outer surface of the vesicles. Therefore, the bare-AgNPs had the only attractive interaction with negative vesicles. These DFM results were well-matched with the interpretation of UV-vis spectra (deviation spectra) and DLVO analysis.

These findings were coherent with the results of *in-vitro*

and *in-vivo* cytotoxicity tests of nanoparticles. Surface charge plays a role in toxicity with cationic surface being more toxic than anionic and neutral surfaces which are most biocompatible, due to the affinity of cationic particles to the negatively charged cell-membrane. Therefore, high zeta potential of nanoparticles is the key factor to stabilize nanoparticles in solutions and is likely to reduce the cytotoxicity.

Conclusions

In summary, we proposed the simple screening method for the analysis of the interaction between several AgNPs (bare-, citrate-, and PVP-coating) and dye-containing DMPG vesicles acting as a biomimetic cell-membrane. This proposed method might be useful for analyzing the cytotoxicity of nanoparticles with cell-membranes *in-vitro*. Negatively charged vesicles had repulsive interactions between neighboring negatively charged AgNPs, such as citrate- and PVP-AgNPs. These interactions (repulsion or attraction) can easily be detected using UV-vis spectra, namely, the absorbance deviation between spectra 4 for mixing of vesicle/x-AgNPs and spectra 5 for simple summation of vesicles and x-AgNPs. If the absorbance deviation is large, particles will be attracted and adsorbed on the vesicle, which is confirmed by DLVO theory. In addition, the DFM scattering image for vesicle/bare-AgNPs showed intense, bright color at the lipid bilayer of vesicle. Therefore, interaction analysis between metallic nanoparticles and vesicles could be measured using UV-vis analysis and DFM. This proof-of-concept test will open the possibility of mimickingcell-membranes (*i.e.* vesicle) to rapidly and conveniently screen for nanotoxicity in other metallic nanoparticles.

Acknowledgments. This work was supported by the Research Grant of Kwangwoon University in 2012 and the National Research Foundation of Korea (NRF-2010-0007050).

References

1. Bhattacharya, S.; Zhang, Q.; Carmichael, P. L.; Boekelheide, K.; Andersen, M. E. *PLoS One* **2011**, *6*, e20887.
2. Krewski,D.; Andersen, M. E.; Mantus, E.; Zeise, L. *Risk Anal.* **2009**, *29*, 474.
3. Andersen, M. E.; Krewski, D. *Toxicol. Sci.* **2009**, *107*, 324.
4. NRC, *Toxicity Testing in the 21st Century: A Vision and a Strategy*; The National Academies Press: Washington, DC, 2007.
5. Marambio-Jones, C.; Hoek, E. M. V. *J. Nanopart. Res.* **2010**, *12*, 1531.
6. Auffan, M.; Rose, J.; Bottero, J. Y.; Lowry, G. V.; Jolivet, J. P.; Wiesner, M. R. *Nat. Nanotech.* **2009**, *4*, 634.
7. Bae, E.; Park, H. J.; Park, J.; Yoon, J.; Kim, Y.; Choi, K.; Yi, J. *Bull. Korean Chem. Soc.* **2011**, *32*, 613.
8. Park, E. J.; Bae, E.; Yi, J.; Kim, Y.; Choi, K.; Lee, S. H. Yoon, J.; Lee, B. C.; Park, K. *Environ. Toxicol. Pharm.* **2010**, *30*, 162.
9. Park, E. J.; Yi, J.; Kim, Y.; Choi, K.; Park, K. *Toxicol. in Vitro* **2010**, *24*, 872.
10. Jan, E.; Byrne, S. J.; Cuddihy, M.; Davies, A. M.; Volkov, Y.; Gun'ko, Y. K.; Kotov, N. A. *ACS Nano* **2008**, *2*, 928.
11. Meng, H.; Xia, T.; George, S.; Nel, A. E. *ACS Nano* **2009**, *3*, 1620.
12. Hirano, A.; Yoshikawa, H.; Matsushita, S.; Yamada, Y.; Shiraki, K. *Langmuir* **2012**, *28*, 3887.
13. Cho, N. J.; Cho, S. J.; Cheong, K. H.; Glenn, J. S.; Frank, C. W. *J. Am. Chem. Soc.* **2007**, *129*, 10050.
14. Chah, S.; Zare, R. N. *Phys. Chem. Chem. Phys.* **2008**, *10*, 3203.
15. Riske, K. A.; Dobereiner, H. G.; Lamy-Freund, M. T. *J. Phys. Chem. B* **2002**, *106*, 239.
16. Bae, E.; Park, H. J.; Lee, J.; Yoon, J.; Kim, Y.; Choi, J.; Park, K.; Choi, K.; Yi, J. *Environ. Toxicol. Chem.* **2010**, *29*, 2154.
17. Song, J. E.; Phenrat, T.; Marinakos, S.; Xiao, Y.; Liu, J.; Wiesner, M. R.; Tilton, R. D.; Lowry, G. V. *Environ. Sci. Technol.* **2011**, *45*, 5988.
18. Moon, J.; Kang, T.; Oh, S.; Hong, S.; Yi, J. *J. Colloid Interf. Sci.* **2006**, *298*, 543.
19. Crow, D. R. *Principles and Applications of Electrochemistry*, 4th ed., Blackie Academic & Professional: New York, 1994.
20. Nieh, M. P.; Harroun, T. A.; Raghunathan, V. A.; Glinka, C. J.; Katsaras, J. *Biophys. J.* **2004**, *86*, 2615.
21. Bhattacharjee, S.; Elimelech, M.; Borkovec, M. *Croact. Chem. Acta* **1998**, *71*, 883.
22. Hiemenz, P. C. *Principles of Colloid and Surface Chemistry*, 2nd Ed., Dekker: New York, 1986.
23. Hsu, J.-P.; Liu, B.-T. *J. Colloid Interf. Sci.* **1998**, *198*, 186.
24. Butt, H. J.; Cappella, B.; Kappl, M. *Surf. Sic. Rep.* **2005**, *59*, 1.
25. Marra, J. *Biophys. J.* **1986**, *50*, 815.
26. Huynh, K. A.; Chen, K. L. *Environ. Sci. Technol.* **2011**, *45*, 5564.
27. Hancock, B. C.; Zografi, G. *Pharm. Res.* **1994**, *11*, 471.
28. Ju, R.; Yong, K.-T.; Roy, I.; Ding, H.; He, S.; Prasad, P. N. *J. Phys. Chem.* **2009**, *113*, 2676.
29. Xu, X.-H. N.; Brownlow, W. J.; Kyriacou, S. V.; Wan, Q.; Viola, J. *J. Biochemistry* **2004**, *43*, 10400.